SpecEye: Towards Pervasive and Privacy-Preserving Screen Exposure Detection in Daily Life

Zhengxiong Li, Aditya Singh Rathore, Baicheng Chen, Chen Song, Zhuolin Yang, Wenyao Xu
University at Buffalo, the State University of New York, Buffalo, New York, USA
{zhengxio,asrathor,baicheng,csong5,zhuoliny,wenyaoxu}@buffalo.edu

ABSTRACT

Digital devices have become a necessity in our daily life, with digital screens acting as a gateway to access a plethora of information present in the underlying device. However, these devices emit visible light through screens where long-term use can lead to significant screen exposure, further influencing users' health. Conventional methods on screen exposure detection (*e.g.*, photo logger) are usually privacy-invasive and expensive, further, require ideal light conditions, which are unattainable in real practice. Considering the light intensity and spectrum vary among different light sources, an effective screen spectrum estimation can provide vital information about screen exposure. To this end, we first investigate the characteristics of the junction between p-type and n-type semiconductor (i.e., PN junction) to sense the spectrum under various conditions. Empirically, we design and implement, SpecEye, an end-to-end, low cost, wearable, and privacy-preserving screen exposure detection system with a mobile application. For validating the performance of our system, we conduct comprehensive experiments with 54 commodity digital screens, at 43 distinct locations, with results showing a base accuracy of 99%, and an equal error rate (EER) approaching 0.80% under the controlled lab setup. Moreover, we assess the reliability, robustness, and performance variation of SpecEye under various real-world circumstances to observe a stable accuracy of 95%. Our real-world study indicates SpecEye is a promising system for screen exposure detection in everyday life.

CCS CONCEPTS

• **Security and privacy → Security in hardware**; • **Hardware**;

KEYWORDS

Screen Exposure; Health; Privacy.

ACM Reference Format:
Zhengxiong Li, Aditya Singh Rathore, Baicheng Chen, Chen Song, Zhuolin Yang, Wenyao Xu. 2019. SpecEye: Towards Pervasive and Privacy-Preserving Screen Exposure Detection in Daily Life. In *The 17th Annual International Conference on Mobile Systems, Applications, and Services (MobiSys '19), June 17–21, 2019, Seoul, Republic of Korea.* ACM, New York, NY, USA, 14 pages. https://doi.org/10.1145/3307334.3326076

MobiSys '19, June 17–21, 2019, Seoul, Republic of Korea

ACM ISBN 978-1-4503-6661-8/19/06…$15.00
https://doi.org/10.1145/3307334.3326076

1 INTRODUCTION

With the proliferation of smart devices, people continue to spend an increasing amount of time looking at the digital screen. Reports reveal that in the United States, adults devote close to 10 hours and 39 minutes every day on various electronic devices such as tablets, smartphones and personal computers [1]. As a medium for information sharing between device and user, digital screens continuously project visible light, a portion of the electromagnetic spectrum, which can be sensed by the human eye. However, long-term exposure to such light, hereafter *screen exposure*, poses vital risks to the user's health. The primary symptoms include disruptions in a circadian cycle as well as the computer vision syndrome [2, 3], which can further lead to the sleep disorder, emotional dysregulation or even cognitive deficit [4, 5]. The corresponding decline in user's productivity leads to an annual loss of more than $63 billion in the U.S. economy [6]. To limit screen exposure, doctors encourage people to periodically relax their eyes by looking away from the digital screen; however, such practice relies on a person's awareness and is ineffective in the real-world scenario.

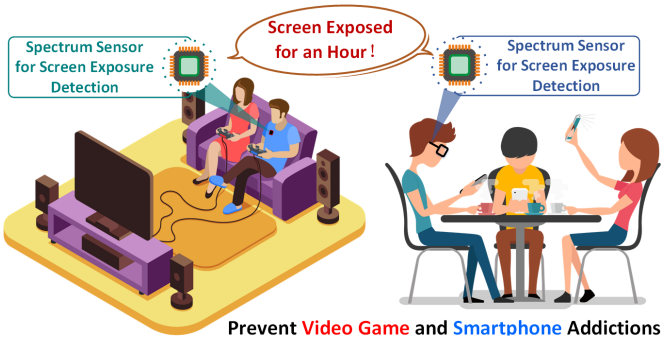

Figure 1: SpecEye utilizes the unique salient spectrum from the screen to enable pervasive screen exposure detection.

How to facilitate a pervasive screen exposure detection has become a challenging, yet intriguing problem. The accepted solution has been to leverage the artificial sign-in/sign-out records or set parental controls [7], both of which can only provide insight into the active period of the electronic device but not the precise period when the user looks at the digital screen. As a result, researchers continue to explore more advanced techniques to govern screen exposure pervasively. The traditional photo life-logs that are employed to capture the ambient environment, are also useful in identifying the presence of digital screens [8, 9]. However, such a technique is significant privacy-intruding as the lifelogging images contain the private information displayed on the digital screen. Even if measures are taken to safeguard the screen content,

camera-based techniques can still leak vital clues about the daily activities of a user. Other methods rely on the use of soft parameters such as screen-to-face distance through the infrared sensor on the smartphone [10–13]; yet, they make strong assumptions about the user's interaction with the electronic device and are unreliable in real-practice. This paper considers breaking away from convention and aims to explore a disruptive approach in monitoring the screen exposure while preserving the privacy of the user.

Research Problem: In this work, the key problem we aim to solve is *how to enable a pervasive and efficient detection of screen exposure from the digital screens without compromising the user's privacy.* Our goal of screen exposure detection arrives with various challenges: (1) Due to its weak intensity, the visible light emitted from digital screens is often submerged with the ambient light. How can we identify the specific salient spectrum in the presence of bright illuminations (*e.g.,* sunlight)? (2) Given the unpredictability in user's interaction with the digital screen, how can we confidently set a uniform rule for screen exposure sensing considering limited information about screen distance, facial direction or screen's brightness levels? (3) One of the prominent concern in the development of wearable technologies is user acceptance. How can we set the design goals to increase the usability of our system in real-world scenarios? We develop practical solutions and address the above challenges in our work.

Our Work: In this paper, we present a novel wearable screen exposure detection system, namely SpecEye as shown in Figure 1, to facilitate screen sensing for the protection of public health. SpecEye offers the following salient features. (1) *Pervasive Detection:* SpecEye works under various conditions (*e.g.*, indoor room, semi-outdoor corridor and outdoor) with different interventions (*e.g.*, chandelier, lamp, and candle), and is capable for inferring screen exposure even in the presence of sunlight. (2) *Privacy Preservation:* In contrast to previous solutions, SpecEye does not record the usage history or statistic application report and is hard to be utilized to infer user activities, thereby preventing the intrusion of user privacy. (3) *Usability:* A user can readily employ SpecEye out-of-the-box as it does not require any user-specific training. SpecEye provides a user-friendly interaction from any position on the facial and chest regions. This allows us to incorporate SpecEye into daily accessories that people are already using on a daily basis, such as eyeglasses and badges.

The foundation of SpecEye rests on the concept of unique spectrum pattern from the screen exposure. Subsequently, we enable a novel sensing modality for non-invasive and cost-effective screen detection by designing and prototyping a wearable ($32mm \times 30mm \times 24mm$), light-weighted ($32g$) and cost-effective (less than $US\$10$) spectrum sensor to probe the projected salient light spectrum. To facilitate the processing of divergent intensities of light signals, we further analyze the *SpecPN signal* (see Section 5.1) and achieve a high-quality sensing signal that is transferred to the smartphone where the feature generation module handles the arbitrary noise in signals. Moreover, we develop a spectrum analyzer, based on a support vector machine (SVM) classifier for robust screen detection under various light conditions. Our extensive evaluation comprising 54 digital screens verifies the sensitivity of SpecEye to sense the screen under different real-world scenarios accurately. More importantly, our system can be immediately deployed in important domains (*e.g.,* educational, industrial, medical) by taking advantage of our interactive mobile application with a personalized graphical user interface (GUI).

The contributions of our work are three-fold:

- We propose a novel method for screen exposure sensing by exploring the salient spectrum. Empirically, we observe that the PN junctions act as a spectrum sensor and reflects the screen exposure with *intrinsic identity* spectrum.
- We develop SpecEye, an end-to-end system for low-cost, non-invasive, and robust spectrum analyzer and further prototype the spectrum sensor. A novel framework is proposed for integration of trace collection in response signal with screen exposure estimation.
- We evaluate SpecEye with different factors including screen types, locations, and time with results showing a base detection rate of 99%. Lastly, a robustness evaluation and real-world study are performed by considering the impact of human and environmental dynamics and other real-life scenarios. In both studies, the system achieved a 95% base accuracy.

2 SPECTRUM PHOTOVOLTAIC EFFECT: CONCEPT AND PRELIMINARIES

2.1 The Concept: Spectrum Photovoltaic Effects of RGB Light

Screen Light Brightness and Spectrum: The light from screens (e.g., smartphones, laptops and televisions) is different from the indoor and outdoor ambient lights from two aspects including the brightness and the spectrum.

Brightness: Screens are designed to be looked and stared by human eyes instead of illuminating the environment. As a result, the brightness level of screen is much lower than the indoor ambient light (*e.g.,* light bulbs and fluorescent lamps), let alone the outdoor ambient light (e.g., sunlight). We use Lux as a measurement unit for light brightness. The brightness of the screen is typically from 0 to 300 Lux [14] while the brightness of indoor and outdoor ambient lights is 800 and $1500Lux$ [15, 16].

Spectrum: At the moment, the two widely used types of digital screens (i.e., LCD and OLED) consist of tiny dots, referred to as pixels, where each pixel is an integration of three primary colors: red, green, and blue (a.k.a, RGB) [17]. Unlike the ambient lights' spectrum covering seven different colors [18], the screen light spectrum is more limited as the R, G, B lights ranged from $620nm$ to $750nm$, $495nm$ to $570nm$, and $400nm$ to $495nm$, respectively [19, 20].

In conclusion, the screen light can be submerged by ambient lights as it has much lower brightness and narrower spectrum. To overcome the challenge, we decide to simplify the analysis space by focusing on only the RGB spectrum which is the entire light spectrum a screen can generate. Noted that we hereby target on only intense ambient light situations (e.g., lights on and daytime) since these are much more challenging for the screen sensing.

Photovoltaic Effects in PN Junction: PN junction (e.g., LED) can be a light receiver capable of capturing an incoming light with a specific wavelength [21, 22]. For example, due to the filtering effects of a colored plastic coating, an LED with red, green or blue coating is only sensitive to the light with the corresponding emission color spectrum. The dominant emission wavelength for RGB

LEDs can be from 625*nm* to 630*nm*, 515*nm* to 520*nm*, and 465*nm* to 470*nm*, respectively [23–25]. And the sensing wavelength of an LED is within a certain range (around tens of nanometers to 100*nm*), which is usually shorter than or equal to their emission wavelength [26, 27]. Being a light sensor, the PN junction relies on the photovoltaic effects, a physicochemical phenomenon which refers to the formation of electric current and voltage in a material upon exposure to light [28, 29]. In other words, it monitors light in the form of voltage change. As demonstrated in Figure 2, a PN junction (i.e., LED) contains a p-type and a n-type materials, where the former contains more free positive charges (i.e., holes) and the latter contains more free negative charges (i.e., electrons). Thus, a electric field exists in the PN junction. While the light shines on the PN junction, photons will knock some electrons off their bonding with holes and generate electron-hole pairs. Due to the existence of electric field, the electron and the hole from each pair moves to the p-type and the n-type materials separately. At the end, a current flow as well as a voltage is generated in the circuit connecting the PN junction.

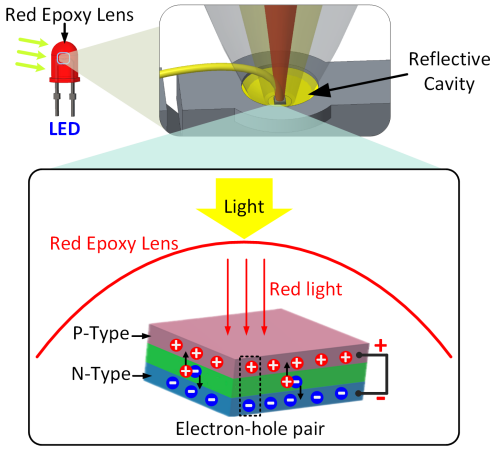

Figure 2: The PN junction (*e.g.*, LED) light sensing mechanism based on photovoltaic effect.

Advantages of Photovoltaic Effects and PN Junction: To justify why the aforementioned approach is a more feasible solution, we compare the photovoltaic effect to other existing sensing rationales as illustrated in Table 1 and the PN junction (e.g., LED and solar cell) to other light sensors as shown in Table 2 (detailed comparison is further explained in Section 11). It is worth to mention that LED is especially superior in terms of color spectrum filtering and high directionality (i.e., the 30-degree 3dB field of view) [30].
Hypothesis: An LED light sensor with RGB colored coatings can mitigate some effects of ambient lights due to its filtering capabilities. Moreover, because of the high directionality of LED light sensor and the vast brightness difference between the screen and the ambient lights, the *SpecPN* signals (i.e., the sensor readings) based on the photovoltaic effects should be distinctly low while directly facing a screen as the sensor is largely covered by the screen light and thus the effects of ambient lights are further minimized.

Table 1: The comparison of four different spectrum sensing mechanisms indicating the overall superiority of photovoltaic effect for spectrum sensing.

	Sensing mechanisms			
	Computer Vision [8, 9]	*Imaging Spectrometer [31]*	*Electromagnetic Emanation [32]*	**Photovoltaic Effect**
Sensing Modality	Camera	Camera	EM Meter	**PN Junction**
Data complicity	Complex	Medium	Complex	**Simple**
Processing time	Long	Long	Medium	**Short**
Input latency	Long	Medium	Medium	**Short**
Scale of equipment	Various	Medium	Large	**Small**
Privacy intruding	Yes	No	No	**No**

Table 2: The comparison of five practical light sensors showing multiple advantages of LED and solar cell against the conventional sensors.

	Light Sensor				
	Photoresistor [33]	*Color Sensor [34]*	*NIR Sensor [35]*	Light-emitting Diode [23–25]	Solar Cell [36]
Cost	Low	Low	High	**Low**	**Low**
Bandwidth range	Long	Long	Short	**Short**	**Long**
Size	Small	Medium	Medium	**Small**	**Small**
Supply power	Yes	Yes	Yes	**No**	**No**
Flexibility	High	Low	Low	**High**	**High**
Setup difficulty	Low	Medium	Medium	**Low**	**Low**
Response time level	ms	ms	ms	**sub-ms**	**ns**

2.2 A Preliminary Study: Spectrum Photovoltaic Effects for Screen Exposure

Proof-of-Concept: We explore the behavior of LEDs under different light sources by analyzing the *SpecPN* signal. Specifically, we aim to determine if the *SpecPN* signal contrasts among the screen exposure from digital screens of three devices and under the light emission from other illumination sources. For proof-of-concept, we employ four PN junctions including R, G, B LED and solar cell, and measure the voltage of the generated response signal between two pins under the influence of light. Figure 3 illustrates the initial response signal in an example scenario considering with-screen and no-screen exposure. Specifically, the subject wearing the sensor

sits facing the desktop monitor (0 to 5-minute interval), then walks outside the room towards the corridor (5 to 10-minute interval). Subsequently, he again faces the laptop screen (10 to 15-minute interval) and then walks along the corridor to the outside environment (15 to 20-minute interval). Afterward, he stares at the smartphone (20 to 25-minute interval) and finally walks around in the outdoor environment for the remaining five minutes. This experiment is repeated three times by three subjects.

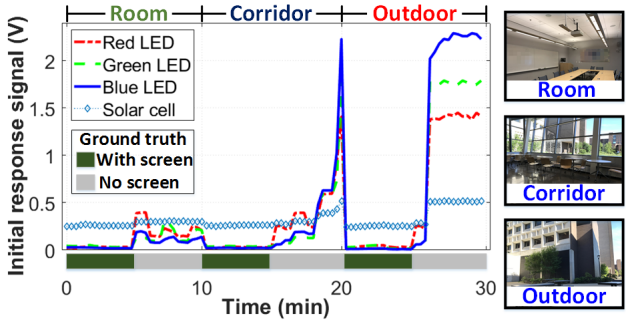

Figure 3: The initial response signal observed under different light spectrum during with-screen and no-screen exposure conditions.

Initial Response Signal: Our results demonstrate that the response signals vary dramatically in no-screen exposure condition; while the intensity of these signals is consistently low when the subject faces the screen. *Naturally, the observed SpecPN signals are distinct between the two conditions and therefore can serve as the identity of the light spectrum for screen exposure detection.* Benefited from its mechanical structure, LEDs can monitor the screen exposure in various scenarios, even under the sunlight, due to their *high directionality*. This allows sensing of the salient spectrum exclusively along the direction that user is facing. In contrast, the solar cell measures a stable response signal with inferior variability between respective conditions. Thus, we can estimate the screen exposure spectrum and regulate the estimation model according to the ambient environment concurrently by leveraging both LEDs and solar cell. We further describe the preliminary methodology to differentiate among the screen exposure spectrum.

Detection based on PN Junctions: As the second phase of our initial assessments, we implement a preliminary *SpecPN signal* estimation system by considering four response signal values as a feature vector to differentiate the signals into two groups, *i.e.,* intra-group (screen exposure) and inter-group (both screen and non-screen exposure). We leverage Euclidean distance, a widely used technique for measuring the feature distance. The feature distance between intra- and inter-groups is illustrated in Figure 4 showing the definite separation between the groups with some overlap. Furthermore, we perform an initial classification on the data using random forests and the results are shown in Figure 5. We notice satisfactory classification performance (92.17% detection accuracy) primarily through the examination of response signal ratio between the solar cell and blue LED, which is consistent with our observations in Figure 3. We continue to explore more advanced features for effectively reducing the overlap and implement a robust classification technique for achieving superior performance and efficiency.

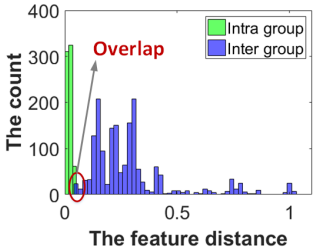

Figure 4: Evaluation of feature distance between intra- and inter-groups.

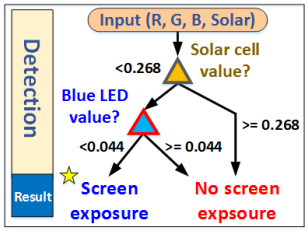

Figure 5: Initial screen exposure detection via response signal of solar cell and blue LED.

Performance Comparison: Lastly, before we completely understand the real performance of the spectrum photovoltaic effects, there is still a consideration of how the real PN junctions' sensing capabilities are compared to the professional off-the-shelf light color sensor. We employ the TCS34725 light color sensor [37], that includes red, green, blue (RGB), and white light color sensor with IR blocking filter for comparison. The spectral sensing ranges of TCS34725 for R, G, B are around from 580*nm* to 650*nm*, 480*nm* to 580*nm*, 400*nm* to 510*nm*, respectively. We repeat the same procedure mentioned in the previous phase and the detection accuracy is 83.5%, which is a little lower than the PN junctions' performance as shown in Figure 6. The leading cause is the light color sensor rejects all the information around the near infrared, which weakens the capacity to sense the ambient environment. Moreover, under the considerations of the electronics price and the power supply, the PN junctions-based solution is more beneficial. These results prove the feasibility of screen exposure detection via PN junctions.

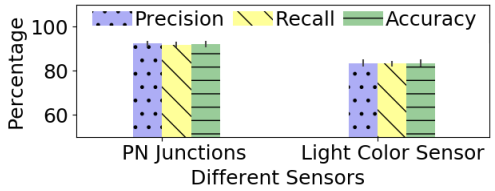

Figure 6: The detection performance comparison between the PN junctions and the off-the-shelf light color sensor.

2.3 Design Challenges

Low-cost and Wearable Spectrum Sensing Modality: It is non-trivial to design a spectrum sensor while ensuring low-cost, compact size, and energy efficiency, especially when the current integrated light sensors require a consistent power supply and possess low flexibility as described in Section 11.

Pervasive Screen Exposure Detection: Taking into account the ambient light, unavoidable variance in signal's scaling as well as diverse intervention sources (*e.g.,* a person crossing between the user and screen), it is challenging to precisely estimate the screen exposure from different screen types while ensuring minimum time complexity.

3 SPECEYE: TOWARDS PRIVACY-PRESERVING SCREEN EXPOSURE DETECTION

We propose a pervasive and privacy-preserving wearable, namely SpecEye, to facilitate the screen exposure detection. The entire system architecture is described in Figure 7. To meet rigorous design requirements, SpecEye employs multiple energy-efficient and extreme -low-cost sensors while providing users with a convenient platform to infer daily screen exposure through a mobile application.

SpecEye Hardware: It adopts the *SpecPN signal* of four PN junctions (*i.e.,* R, G, B LED and solar cell) to reflect the salient spectrum and infer the light condition. The system time clock is leveraged to assist the detection.

SpecEye Software: It comprises signal demodulation and preprocessing scheme to filter the light/thermal noise and extract relevant features, ultimately transmitting them to the mobile application. The screen sensing model is established based on the selected features and the trace is fed into an adaptive screen exposure estimation model to obtain the detection result.

We further describe the intricate design details of each utilized component in the following sections.

4 A WEARABLE AND COST-EFFECTIVE SPECTRUM SENSOR DESIGN

The spectrum sensor, shown in Figure 8, comprises two primary modules: (1) PN junction; (2) microprocessor control unit (MCU) and wireless radio-frequency (RF) Bluetooth module. In the scenario when user is facing the digital screen, the PN junction measures the light emitted from the screen while the MCU with Bluetooth module feedbacks the resulting *SpecPN signal* to the mobile application.

For the PN junction, we select off-the-shelf R, G, B LEDs and solar cell which are self-powered while functioning [23–25, 36]. To simultaneously achieve the spectrum sensing and establish an accessible wireless link between the spectrum sensor and spectrum analyzer, we adopt RFduino with BLE 4.0 and ARM Cortex. The RFduino is designed on Bluetooth 4.0 with additional characteristics including energy efficient, finger-tip size, compatibility with Arduino, wireless-enabled microcontroller and low-cost [38]. The MCU and RF component is based on 16MHZ ARM Cortex M0 with 128KB Flash and 8KB RAM. The supply voltage is 3V and the working current is 18mA. The Bluetooth component enables transmission of ASCII data back and forth between the spectrum sensor and the spectrum analyzer. The communication data package and direction can be customized while the communication distance can be more than 10m, further supporting the system's usability. On the board, the P-type pin of PN junctions are connected to the ground pin while the N-type is connected to the general-purpose input/output (GPIO) pin, *i.e.,* from 3 to 6, of RFduino. Besides, the Serial Peripheral Interface Clock (SCK) pin and Master Out, Slave In (MOSI) pin is established, which controls the synchronization clock and manipulate the data to be transferred to the mobile application after the connection, receptively.

5 SPECTRUM ANALYZER FOR SCREEN EXPOSURE

5.1 SpecPN Signal Demodulation

As we previously mentioned in Section 2.2, an overlap is observed during separation of respective intra- and inter-groups when the initial response signal is assumed as a feature. The primary reason is due to the sensitivity of initial generated signal from LED to circuit load and ambient light. Therefore, for achieving superior detection results, it is essential to demodulate the raw signal and explore the capacitance in PN junction to aid in the investigation of advanced features.

SpecPN Signal*:** When a diode is connected in a reverse bias condition (μs level duration), *i.e.,* a positive voltage is applied to the N-type material and a negative voltage (or ground) to the P-type material, the positive voltage applied to the N-type material attracts electrons towards the positive electrode and away from the junction. Meanwhile, the holes in the P-type end are also attracted away from the junction towards the negative electrode. The net result leads to the depletion layer growing wider from a lack of electrons and holes, further implying that the PN junction can be treated equivalently to a capacitance [39]. When the photons collide with the wider depletion zone, they could generate sufficient energy to maneuver the electrons until the respective zone is back to the initial condition. The generation time τ (as shown in Equation 1,2) is related to the photons volume (light brightness). Besides, it is widely acknowledged that capacity has the trait of filtering the circuit noise and making the generated voltage stable and efficient [40, 41]. *In conclusion, we model the spectrum light response signal based on capacitance in the PN junction under the photovoltaic effect, as* ***SpecPN signal:

$$V_c = -R\frac{d}{dt}(C_s V_c), \tag{1}$$

$$\tau = 1 - e^{-W} + J(\eta, W). \tag{2}$$

Practical Measurement of *SpecPN Signal*: In Equation 1, R is the internal equivalent resistor in LED, C_s is the resulting static capacitance, V_c is the potential across the PN junction. In Equation 2, V_0 is initial applied direct potential to build up a space charge, $J(\eta, W)$ is an integral related with V_c and V_0, W is the linear combination of V_c and V_0. Considering C_s and V_c are decided by LED property and incident light respectively, we can differentiate light intensities by recording the discharging time of LED, when we keep V_0 constant for each time as shown in **Algorithm 1**.

5.2 SpecPN Signal Preprocessing

Due to the unavoidable variation in light sensing, we develop a signal pre-processing algorithm to obtain the relevant light information after the signal modulation. Other unrelated information, such as light noise and thermal noise, which are further removed. Considering we have exploited the capacity merits during the primary phase of light sensing in Section 5.1, a Median filter is applied to eliminate the mentioned noises. The reason is that these noises are large pulse interferences from accidental factors in the external environment or the internal instability of the circuit. A Median filter continuously samples for N times, sorting the N times of

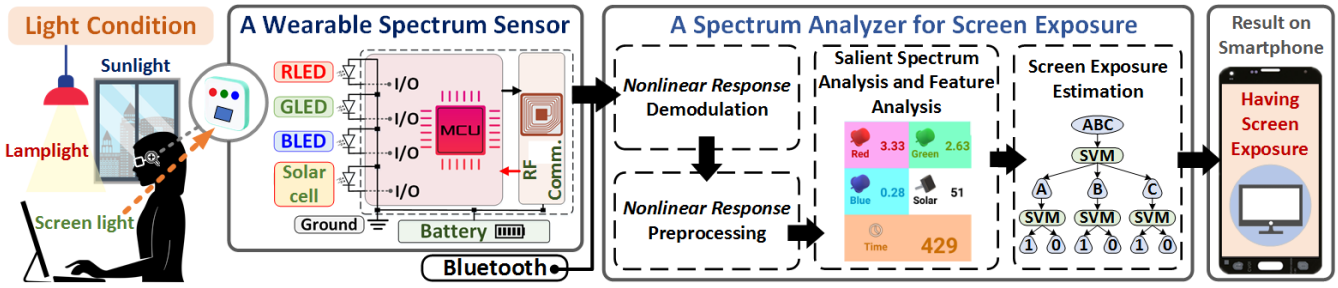

Figure 7: The system architecture of SpecEye, mainly consists of a wearable spectrum sensor to sense the salient light spectrum from digital screen and relay the *SpecPN signal* signals to a spectrum analyzer for estimating the screen exposure. Real-time results of screen exposure are accessible to the user through a mobile application.

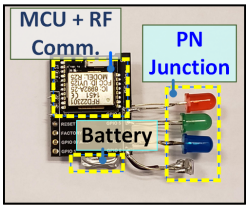

Figure 8: The hardware design of wearable spectrum sensor with PN junctions to capture the light spectrum, and MCU and RF communication channel to feedback the *SpecPN signal*.

sampling values by size and taking the middle value as the current effective value, which can effectively overcome this fluctuation interference [42]. Additionally, compared to other widely used filters (*e.g.*, Kalman filter), this approach is computationally lightweight [43].

Algorithm 1 *SpecPN Signal* Demodulation

Input: $Led\_N(t)$: The stream of the measured signal on the LED N type side leg
$System\_Time()$: The system time in sensor
Output: τ: The modulation signal on PN junction

```
T_pre ← System_Time()                          ▷ Get the start time
PinLedN ← 1                                    ▷ Apply reverse bias to N-type pin
j ← 0                                          ▷ Init the parameter
do
    PinLedN ← Input(Led_N(t))                  ▷ Begin to measure the generated signal form the PN junction
while PinLedN == 0
T_cur ← System_Time()                          ▷ Get the end time
τ = Normalize(T_cur − T_pre)                   ▷ Get the discharge time in the test
return τ;
```

5.3 Salient Spectrum and Feature Analysis

Feature extraction has the potential to enhance the robustness and efficiency of the screen exposure sensing model. Therefore, we exploit the inherent traits in the *SpecPN signal* to the salient spectrum. Considering the light from the screen comes from the three basic sub-pixels, red, green and blue, we select these three color light as the salient spectrum sensed by red, green and blue LEDs correspondingly. Besides the demodulation signal from the LED, we also utilize the potential across the solar cell. For each time, we acquire the discharge time of three LEDs (red, green, blue) and one solar cell response signal successively, with the total sensing time of these four PN junctions, as the *features*.

Figure 9 shows an example of spectrum sensing under 10 different viewing contexts performed in a lab environment. The first five contexts involve directly facing the screen (Dell 24 Monitor: P2417H [44]) with specific interfaces as the red image, green image, blue image, default Google search page, and empty Word page. The remaining five do not require a screen while facing the ceiling, floor, and surrounding walls. It can be observed that different sensing contents have different features values, implying that *these five features of the signal can be treated as the distinctive identity of light with or without the screen exposure condition*. Moreover, the ratios among red, green and blue LEDs in contents without screen exposure are more stable compared to those that include the screen exposure. A similar situation with Section 2.2 is observed for the rate between LEDs and the solar cell; the rate is much higher when the subject is not suffering from screen exposure. These scenarios may help us to better understand the screen exposure and design a screen exposure detection system.

5.4 Screen Exposure Estimation

In this section, we establish a lightweight model on a mobile device to detect the screen exposure more accurately and robustly. This step is critical in order to achieve better performance in our system.

Trace Collection for Model: After refining, a set of five feature values (i.e., red, green, blue, solar and generation time) for each time are treated as a ***cycle***. Intuitively, the screen sensing signal with more cycles will contain more unique characteristics of the light and thereby achieve better detection performance. Thus, we set M continuous *cycles* as a ***trace***, which is fed into the screen exposure detection as described in Algorithm 2. However, more *cycles* within a *trace* can increase the computation overhead. To balance this trade-off, we empirically choose $M = 3$ and the corresponding original sensing time within 0.9s (we further evaluate the sensitivity of M in Section 7.2).

Adaptive Screen Exposure Detection: As the spectrum varies significantly at different places, it is difficult to confidently set a

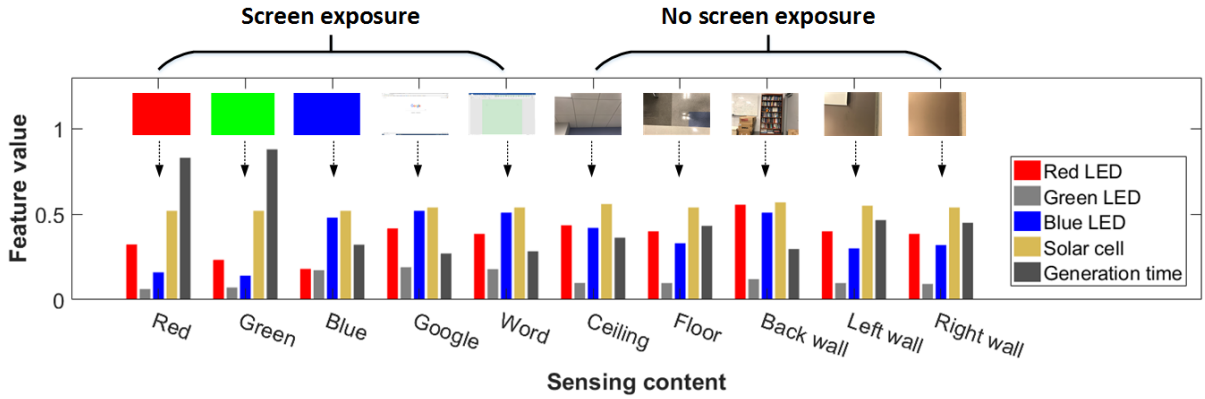

Figure 9: An illustration of *SpecPN signal* after demodulation under with and without screen exposure conditions. It can be observed that the feature values are different for different screen contents, implying the feasibility of using these five features as a distinct identity of the light spectrum.

uniform rule for screen exposure sensing estimation. In our work, we employ adaptive screen exposure classification [45] where two supervised learning layers are used to detect if a screen is sensed, beginning with a training phase and followed by testing (or classification). The classification model is further described in *Algorithm 2*. In practice, the first layer classifies the tested trace into each pre-trained class of environment *e.g.*, indoor, semi-outdoor and outdoor. Afterward, the second layer classification, which is designed for one location selected by the first layer result, shows the result if the user faces the screen with the same input tested trace. During the training of each classier, n traces of screen exposure sensing signals from each sensing content are collected. For m sensing contents in the database (namely, m pre-registered classes), $n \times m$ feature vectors are used to train the classifier altogether. In SpecEye, we employ SVM while the Gaussian radial basis function is selected as the kernel function to map the original data to a higher dimensional space. During the testing phase, SpecEye collects a trace which acts as an input for the dual layer SVM model to generate the probability set of classifying the corresponding test trace into each pre-trained class.

Algorithm 2 Adaptive Screen Exposure Detection Model

Input: $cycle(t)$: The tth *cycle* of four features from the sensing device

Output: $C(i)$: A judgment if the device at tth *cycle* faces the screen

1: $C_i \leftarrow 0$; $trace(t) \leftarrow 0$; ▷ Init the parameter
2: $trace(i) = [cycle(t), cycle(t+1), cycle(t+2)]$; %Classifier:
3: **for** $i \in \{1, \ldots, K\}$ **do**
$L(i) = Classify1(trace(i))$; ▷ (1st layer) Classify each trace and get the predicted environment
$C(i) = Classify2forL(i)(trace(i))$; ▷ (2nd layer) Classify each trace and get the predicted result
4: **end for**
5: **return** $C(i)$;

Table 3: Runtime of all components in the SpecEye system.

Typical LED detector	Typical Solar cell detector	Bluetooth communication	I/O Blocking	Detection application	Total delay
271.3ms	0.3ms	36.7ms	0.7ms	590.5ms	899.8ms

6 THE PROTOTYPE IMPLEMENTATION AND EVALUATION SETUP

6.1 SpecEye Implementation

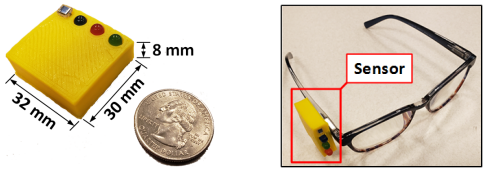

(a) (b)

Figure 10: Our prototype of SpecEye is (a) lightweight with size similar to US quarter coin and (b) can be integrated with daily accessories such as eyeglasses.

6.1.1 Sensing Modality: Sensing Hardware Implementation. During the design of a wearable spectrum sensor, energy efficiency and ultra-low cost are fundamental yet challenging principles that must be satisfied. To this end, we design and prototype a wearable sensor by 3D printing, whose size is *32 mm* × *30 mm* × *24 mm* (*1.26 inch* × *1.18 inch* × *0.94 inch*) and the weight is *32 g* (1.1 oz). The supply voltage is 3 V and the working current is 18 mA. Figure 10 depicts our sensor prototype standalone and attached to a pair of eyeglasses, indicating SpecEye's wearable feature. To reduce the communication workload and save the battery energy, the sensing data is batched on the MCU and then periodically transmitted to the phone.

6.1.2 Applications Design on Smartphone. To provide vital information to the users about their current light condition and daily

screen exposure, we implement the upper application as an APP on the smartphone. Figure 11 describes two interfaces showing the screen detection result when the user suffers from screen exposure and the screen exposure time. Overall screen time is also provided to alert the user suffering from long-term exposure.

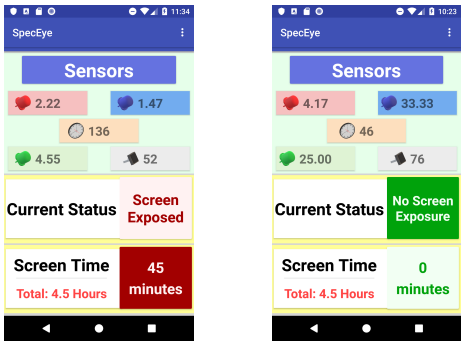

(a) (b)

Figure 11: (a) and (b) shows the GUI interfaces on the smartphone notifying the user about the screen exposure.

6.2 Usability Analysis

As a wearable system, SpecEye requires the user to wear a spectrum sensor. To provide superior usability and user experience in real-world application, we design SpecEye to allow its effortless integration into existing accessories that the users are already comfortable using in their daily lives [46, 47]. Our prototype supports two scenarios: badges, and eyeglasses. Figure 12 shows the relative positions of the device in each scenario. While SpecEye performs well on all facial areas, shoulders, and the sternal surface, we focus on these two positions since they conform with the popular accessories that have received immense user acceptance in the real-world [48, 49]. All participants in our study demonstrate the willingness to accept the different configurations of SpecEye, when they are well-educated about the healthcare implications of the screen exposure. And they all feel reminders from SpecEye is reasonable and helpful.

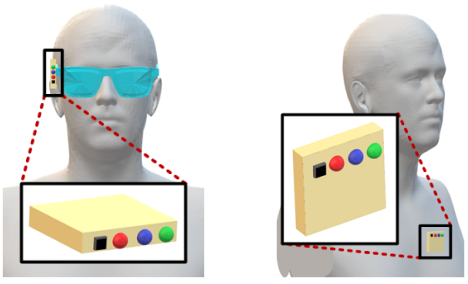

(a) (b)

Figure 12: The two popular wearable scenarios supported by SpecEye: (a) wear on the common eyeglass and (b) wear as the badge.

6.3 Delay Overhead Analysis

System Delay Characterization: To satisfy the demanded practicality and effectiveness in a real-world deployment, it is crucial for the system to have a minimized delay for ensuring no adverse impact on the detection process. In this section, we investigate the time efficiency of SpecEye. We collect the one-hour runtime information of all the components in the SpecEye system, including the sensor response of the transforming light signal. This experiment is conducted without other applications running in the background. The average result for each connection is listed in Table 3. We observe that the total delay of SpecEye is about 899.8ms, which is rapid enough to implement continuous screen detection for a digital device user. Another important observation is that the detection application consumes the majority of runtime by 65.6%. Other consumptions are primarily due to hardware-level operations such as the photoelectric energy format transforming and signal communication.

Screen Exposure Detection Runtime Breakdown: A smartphone, *i.e.,* Galaxy S9+ with an ARM Cortex A-55 core [50], is employed to further evaluate the system overhead. The detailed runtime breakdown information is shown in Figure 13. We can observe that the computing of the screen exposure detection algorithm (*i.e.,* signal modulation and classification) is the bottleneck with 87.2% proportion compared to the overall 12.8% from AD conversion, memory, and IO. It is worth mentioning that this phenomenon provides us with a direction to optimize the detection process and further improve the system performance.

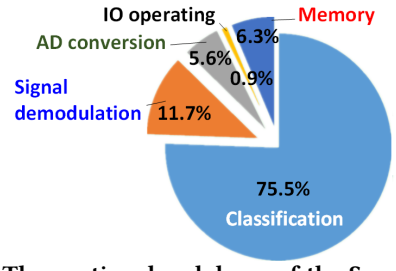

Figure 13: The runtime breakdown of the SpecEye application on the smartphone.

6.4 Test-bench Preparation

In this section, we describe the experimental setup and performance metrics utilized for the evaluation.

Screen Type and Mode: As shown in Figure 14, we select five types of screen exposure sources, including smartphone, tablet, laptop, display, and TV [51] that are used daily in a typical lifestyle. To extensively evaluate every possible form of screen exposure, we recruit 54 screens comprising 15 smartphones, 13 displays, nine tablets, 14 laptops, and three TVs. Among these, 46 screens are of LCD type while the rest are OLED. The screens are well functioning with no defects. Their sizes vary between 3.5 inches to 70 inches while the usage time ranges from 1 to 8 years.

Data Collection: We recruit five subjects, three men and two women, to wear our SpecEye system for participating in the evaluation. It is ensured that every participant follows the host institute internal review board protocol. All signals are acquired in 43 different locations under different weather conditions, including sunny, cloudy, and rainy days and at different times of the day (8:00-22:00) for two weeks as shown in Figure 15. In other words, it contains

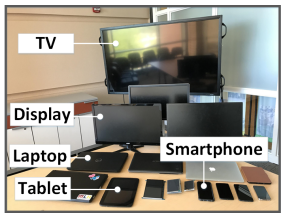

Figure 14: Commodity screens from different devices in our study.

Figure 15: Different test locations in our database.

the scenario where the ambient light can be weak or strong. The studied sites involve 16 indoor locations (*e.g.*, rooms, homes, shopping mall), 13 semi-outdoor locations (*e.g.*, corridors, halls) and 14 outdoor locations (*e.g.*, outdoor campus, football fields and downtown squares). For each participant, each location is visited once every two days. They are staggered throughout the day. During the subject's presence at these locations, SpecEye system performs continuous detection for the experimental sites throughout the entire time. For each site, the users are instructed to watch the screen for two minutes and then look at surroundings for another two minutes. These two steps are repeated for five times. It is important to note that these sites are different from the environments where we collect the prior data and learn the screen sensing characterization. The total size of the Data Collection is 30,100 traces, in which half traces are with screen exposure while the rest are not. Among these traces, 21,070 are utilized for training, and 9,030 for testing.

Performance Metric: In our experiments, we use the true positive rate (TPR), false positive rate (FPR), equal error rate (EER) and receiver operating characteristic (ROC) as the evaluating metrics in the overall performance analysis [52]. The lower the EER is, the better the system's performance. Besides, it is natural to employ Accuracy, Precision and Recall as detection system metrics [53].

7 SPECEYE SYSTEM PERFORMANCE

To maximize the efficiency of SpecEye for detection of the screen exposure from various light conditions, it is crucial to analyze the variability in performance with respect to trace length and redefine the model, if required. We further evaluate the overall effectiveness of our proposed system.

7.1 Overall Performance of Screen Exposure Detection

For the overall performance analysis, the data is acquired from the database, namely Data Collection, built using our sensing system. We repeat the experiment 10 times and calculate the average performance. In addition, to verify if our feature dataset can be further reduced, we perform a comparison with the utilized single PN junction exclusively. The results, in terms of TPR, FPR and EER, are presented in Figure 16. The EER of the entire system based on SVM is 0.80% while its accuracy is up to 99.29%, concluding that our method is feasible and more importantly, effective, for screen exposure sensing while achieving exceptional accuracy. The EER of specific conditions which involve the use of LED features is all less than 10% while their accuracy is higher than 90%, which matches the analysis in Section 2.2. This result validates that our system has a better performance due to our novel signal modulation based on *SpecPN signal* design in Section 4.

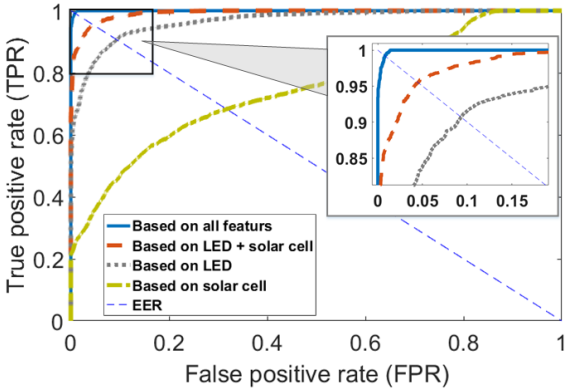

Figure 16: The overall system performance with different features.

7.2 Impact of Trace Length

As discussed in Section 5.4, in this experiment, we investigate the influence of trace length on the performance of SpecEye with different *cycles*. We start with the trace of one *cycle* and increase the number gradually. The precision and recall for each test trace are described in Figure 17. It is observed that the classification precision increases from 95.11% to 99.64%, with the *cycles* growing from one to three. Afterward, a turning point appears and the precision/recall keep around 99.7%, when the *cycles* raise to five. The variation of the precision/recall decreases with the increase in the number of *cycles*. Therefore, we select the *cycles* limit as three for a trace (15 dimensions) in our system.

8 ROBUSTNESS EVALUATION

In real practice, the ambient environment can be a detriment to the performance of the system by introducing arbitrary noise or adversely interfere with the probe hardware operation. We consider several factors evident in daily life and evaluate the robustness of SpecEye against human and environmental factors.

8.1 The impact of The User

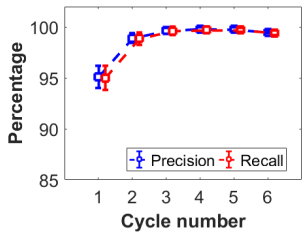

Figure 17: Evaluation with different cycles for a trace.

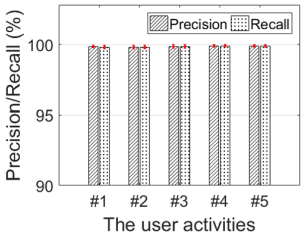

Figure 18: Evaluation with different user activities.

8.1.1 Effect of Motion. During routine usage of electronic devices, it is common that the user is not keeping a standard gesture before the screen for an extensive period and changes position to minimize the physiological strains. To verify if the system could accurately

sense nonetheless, we design five commonly performed activities (noted as #).

- **# 1:** sit facing the screen for 5 minutes and then stand looking at the direction of ceiling for 5 minutes.
- **# 2:** sit facing the screen for 5 minutes and then walk around in the room for 5 minutes.
- **# 3:** sit facing the screen for 5 minutes and then walk outside the room along the corridor for 5 minutes.
- **# 4:** walk along the corridor for 5 minutes and then sit facing the screen for 5 minutes.
- **# 5:** walk around the room for 5 minutes and then sit facing the screen for 5 minutes.

Five participants repeat these activities for five times and these traces are used as the test set against the model trained in the Data Collection. The result described in Figure 18 indicates both the precision and recall to be above 99%. Therefore, the performance of the SpecEye system remains unaffected.

8.1.2 Effect of Sensing Distance. The distance between the screen and user depends upon various factors, such as screen size, usability and even the user's eyesight. To evaluate the influence of sensing distance on the system, we conduct the following experiment. Five participants look at the screen from four different distances. The acquired traces are used as the test set against the model trained in the Data Collection. The result is shown in Figure 19. We observe that both precision and recall are above 99.6%, indicating the optimal usability of our system in satisfying different application requirements.

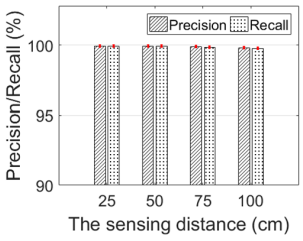

Figure 19: Evaluation with different sensing distances.

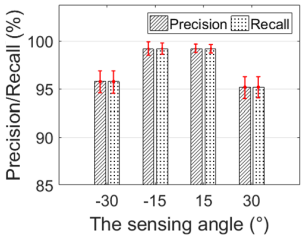

Figure 20: Evaluation with different sensing angles.

8.1.3 Effect of Sensing Angle. During real-world application, it is infeasible for the user to continuously face the screen at a fixed angle due to physiological constraints, activities requiring body movement or analyzing information from different areas of the screen. We examine the effect of sensing angle by asking the five participants to look at the screen from four different angles at the depression and elevation angle ((-) and (+) represent the depression and elevation direction respectively), thereby obtaining the traces as samples for testing. Figure 20 demonstrates the observed precision and recall as above 95.2%. The performance drops severely after 30 degrees due to the LED sensitivity view limited by the current LED manufacture technology. However, the primary screen viewing angle is from 3° to 20° [54], within our sensing range. The performance of SpecEye remains unaffected.

8.2 The Impact of Ambient Environment

Several environmental factors such as screen brightness, ambient light and temperature pose non-trivial challenges in the sensing field, especially in scenarios involving light sensing. In this section, we investigate the impact of these three effects on SpecEye, repeating 10 times for each test.

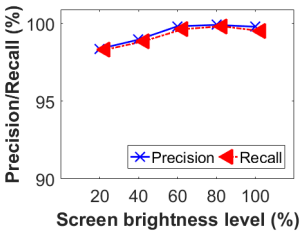

Figure 21: Evaluation under screen brightness levels.

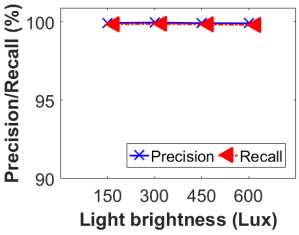

Figure 22: Evaluation under varying light brightness.

8.2.1 Different Screen Light Brightness. It is a fact that different users have distinct brightness settings for their screens depending upon the user's preference or device battery life. In this experiment, we first identify the light by the radiation intensity of illumination from he screen. We employ 10 smartphones and 10 displays and set corresponding brightness levels at 20%, 40%, 60%, 80% and 100%. For smartphone, the viewing distance is set at 35cm and for display, it is 70cm. Five participants look at each screen with 10 different contents. The acquired traces are used as the test set against the model trained in the Data Collection. Learned from Figure 21, both precision and recall are higher than 98.3% in every case. The performance rises with the increase of screen brightness and remains constant (around 99%) when the brightness reaches 60%.

Screen Dim Condition: In the scenario when the user watches a movie using an electronic device (e.g., the laptop), it is not uncommon for the background of the screen to be considerably dim, or at times completely dark. Tradition solutions (i.e., the optical-based) are hard to handle this issue, because the dim screen is usually misdiagnosed as the dark place. However, we evaluate this condition to observe that the precision and recall are higher than 98.1%, further implying the limited effect of screen light brightness on our proposed system.

8.2.2 Location Light Intensities. For different locations or time during a day, the light intensity in the user's habitat may vary depending on the auxiliary influence from other light sources. To determine the effect of light intensity on the system performance, we select three multimedia conference rooms and set different light brightnesses of the room with an illumination of 150, 300, 450 and 600Lux, which is the proper illumination range for watching [55]. As shown in Figure 22, the precision and recall are all above 99.9%, further implying the robustness of SpecEye against surrounding light intensity.

8.2.3 Temperature Impact. Considering the existing temperature drift on the sensor, we conduct the experiment to verify if the location temperature has any adverse influence. We select three different locations and set different temperature of the location from 10 to 30°C. The precision and recall, mentioned in Figure

24, are higher than 99.1% during the respective variations which implies that SpecEye possesses strong tolerance to temperature fluctuation and is immediately deployable in different environment or weather conditions.

8.2.4 Ecological Environment. In real practice, the ecological environment of the usage may vary considerably. We consider common diverse settings in the daily workplace in terms of screen factors and ambient factors. Typically, we select four conditions where (1) the screen is set at the night shift mode (e.g., Macbook Pro) under the normal illumination; (2) the hue light tube has three color modes (e.g., red, blue and green); (3) A desk reading lamp with cool and warm white color Light; (4) contains mixed ambient light sources (e.g., sunlight, one LED lamp and one fluorescent light bulb). From (2) to (4), the screen is set under the default mode. Specifically, we try every possibility under each condition. Again, we evaluate the above four conditions. Figure 23 demonstrates that their performances all achieve above 99.02%. In conclusion, SpecEye presents strong robustness to different light environments.

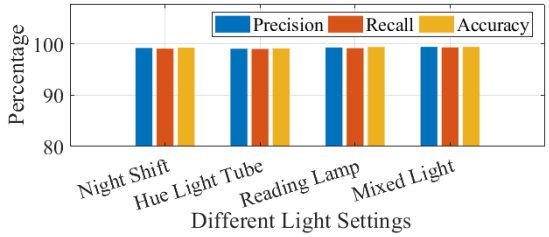

Figure 23: Evaluation under different light settings.

9 REAL-WORLD STUDY

In this section, we conduct a real-world study by applying SpecEye for screen detection in various situations. It is important to prove the permanence of a practical application. We first introduce our experimental setup to further examine the screen detection accuracy of our system during real-world applications.

9.1 Experimental Setup

Besides the human dynamics or the environmental factors, another significant aspect in daily life that leads to variability in the amount of screen exposure is the user's job. We enroll five subjects (three males and two females) to participate in the longitudinal study lasting 30 days. The subjects comprise of people working in different professions including two university students, one professor, one homemaker, and one accountant. Every volunteer wears the system from 8am to 8pm. For the ground truth, we use a camera life logger [56] to record their activities. This wearable camera takes one picture per minute. Finally, we collect 5400 samples by randomly selecting sampling points, and manually validate detection results.

9.2 Test Accuracy

Time Impact: For 30-day duration, we observe the mean values of accuracy between 95% and 96% and the variations among 1.5% and 1.6%, further depicted in Figure 25. We conclude that accuracy has no significant performance decrease or ascending tendency against time change. Furthermore, it demonstrates superior performance in contrast to a method utilizing narrative clip with a 26.3% accuracy improvement [8].

Emerging Light Condition Impact: In daily life, considering that light condition is diverse in weather, indoor illumination, and other sources affected by absorption, refraction, and reflection effects, the mix of light flow may appear similar as the light from the screen, not to mention there might be new types of light decoration emerging from time to time.

The Effect of User Habits: Finally, we check the users' working and living habits, and their impacts on the system. Different occupations may face different light conditions at different locations with different activities at different times. Even two university students can have completely different schedules. We find our system can be applied to various occupations, no deterioration performance is found with any participant.

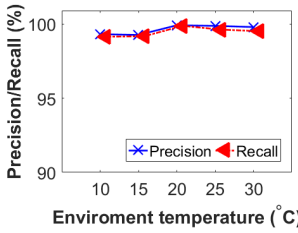

Figure 24: Evaluation under environment temperatures.

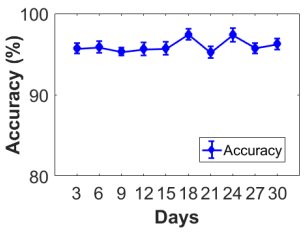

Figure 25: Evaluation under 30 days real-world study.

10 DISCUSSION

10.1 System Limitations

Although the current SpecEye realizes screen exposure detection, considerable efforts are still needed before it can be practically deployed. The major concerning of SpecEye is that the weight of the device is inevitable higher than the ordinary glasses, which makes it uncomfortable for long-time wearing. Thus, we plan to lessen the wearable sensor in the next version by removing the battery and the BLE module and just keeping the PN junctions. Considering 5G technology is coming and the first-generation smartphone equipping 5G baseband is introduced to the market, we utilize the backscatter [57] or solar cell [58, 59] based solutions to power the communication with the new wearable sensor. Also, we notice the system has a limited sensing performance when the user watches the screen from an oblique view, which will lay the foundation to improve the current design. Furthermore, as a first exploration paper on the sensing device approach for screen exposure detection, some limitations exist in the application assumptions. We consider that the user is exposed to the screen for a long time when he is within a common distance from the digital device (*e.g.*, the smartphone, monitor and 70*in* TV viewing distance are from 9.9 to 32.9*cm* [60], from 50 to 100*cm* [61] and from 177 to 266*cm* [62] respectively). The sudden motion changes, (*e.g.*, a glance at the screen), having only little exposure, are excluded in our system consideration. Besides, we assume the user watches the screen under the common scenarios, placing the monitor at a right angle or preventing from the glare and bright light directly behind the screen [63]. We will refurbish the system in the next version based on these limitations.

10.2 Sensing System Optimization

Wireless Communication: The communication distance is an important factor for practical application. In our system, the communication distance between the sensing device and the smartphone is more than 10m with obstacles (*e.g., human, wall*), which satisfies most situations. However, there is some latency in communication, especially in initial connection establishment. Although some advanced wireless communication technology is not well developed, there is an abundant amount of research in this field, and these sources are being constantly improved. They could be incorporated into our system to replace the current Bluetooth module when they have been made powerful enough.

Commodity Exploration: For this paper, we utilize three LEDs and one solar cell to detect the screen exposure, which is economical and widely available. We could scale up its working scope of sensing multi situations with more PN junctions forming a sensing array to further improve its resolution. Specialized LED and solar cells with shorter rise/response time can be applied in the same design for achieving superior performance. However, with increasing the sensing device size or advanced PN junction, fabrication cost and complexity grow. By removing the need for specialized light sensors that are costly and not widely deployed, we push SpecEye design to maximal efficiency and lower its practical barrier to be adopted in practice.

10.3 SpecEye for Future Applications

Agriculture: Considering our system can provide functional and structural sensing of the light spectrum with multiply PN junctions, it holds the opportunity to be a powerful tool of fruit or vegetables ripeness detection and quality testing [64]. Although it is still in its infancy, we can see there is a bright outlook for emerging light spectrum applications in agriculture.

Medical and Healthcare: As the technology of electronic devices continues to integrate with every aspect of human life, it is vital for the medical and healthcare domains to minimize negatives effects by innovative researching techniques. The evolution of optical spectrometry makes a great effort to address these issues through novel concepts that directly link biological activity to spectrometer signal, which naturally matches with our system [65].

Environmental Monitoring: Nowadays, researchers start to utilize imaging spectrometer for environmental monitoring, such as sensing ocean (or lake) water-color and measuring plant reflectance light [31]. In future, our system can be applied to these fields.

11 RELATED WORK

Spectrum Estimation: To better illustrate the fundamental mechanism, Table 1 describes the comparison among four representative spectrum sensing mechanisms. Computer vision techniques and imaging spectrometer require a significant amount of resources for data processing [8, 9, 12, 31, 65]. More importantly, the camera-based techniques are not privacy-preserving as they can leak user's private information through captured images. Meanwhile, the sensing device needed for detecting electromagnetic (EM) emanations is typically bulky and expensive [32]. Therefore, we utilize the photovoltaic effect on PN junction to sense the spectrum without compromising the user's privacy. A comprehensive evaluation of five widely-used PN junction sensors is shown in Table 2. Photoresistor requires additional supply power to reflect the light signal [33]. Both the integrated light color sensor [34] and NIR sensor [35] are constrained by the restricted flexibility following the strict protocol. More importantly, a photoresistor can only sense the light intensity over the whole spectrum in the ambient environment, which is not sufficient to differentiate the specific light from the digital screen. Notably, the light color sensor [34] is an admirable alternative as mentioned in Section 2.2 and the system design and principles can still be utilized when a color sensor is used for prototype implementation. Thus, we select PN junction (*i.e.* LED and solar cell) to sense the screen exposure spectrum, through development of an ultra-low cost, privacy-preserving and energy efficient wearable system.

Screen Exposure Detection: Detecting the screen to infer its exposure is an emerging topic. In [66], Wahl *et al.* designed a smart eyeglasses to detect the computer screen. However, it only works under the ideal condition below 200lux light intensity, which is not practical in daily life. A related thought is to directly detect the period of facing the screens. In [8, 9], Fan *et al.* employed computer vision to detect digital screens in photo lifelogs. However, this method is based on the off-line monitoring and quite sensitive to the ambient environment. Besides, the screen exposure can be inferred from the screen or device log. In 2011, Cajochen *et al.* proposed to design a computer screen with a profile that can be add timed, essential light information [2]. The iOS and Android support a built-in screen time feature to manage the screen time [67, 68]. However, they are about the screen working time, not the screen exposure time for the user. Moreover, the recorded results can be utilized to breach user's privacy.

PN Junction applications: In the last decade, many researchers have explored the PN junction for application in diverse fields. In [69], Zhao *et al.* propose a visible light communication system in the dark by LED. In 2017, Tauhidur *et al.* achieve LED-camera communication using superposed reflection light [70]. The PN junction is also applied in characterizing the nutrients and detecting adulterants in liquid food with the photoacoustic effect [71]. Besides, increasing amount of studies utilize the PN junction in indoor localization [72], micro-sensing and quality assurance [73] and visual privacy protection against the mobile camera [74].

12 CONCLUSION

In this paper, we proposed a screen exposure detection system SpecEye to remind the user about the screen exposure time in daily life, an attempt to reduce the screen exposure impacts. We started from the spectrum analysis of the screen exposure. Then, we proposed a wearable spectrum sensor and a spectrum analyzer to detect the screen exposure accurately. Furthermore, extensive experiments indicated that our SpecEye can achieve more than 95% accuracy in less than 0.9s within the daily viewing range. Different levels of evaluation confirmed the reliability, and robustness of our proposed system. The research findings are an essential step for neutralizing the screen exposure.

ACKNOWLEDGMENTS

We thank our shepherd, Dr. Xia Zhou, and all anonymous reviewers for their insightful comments on this paper.

REFERENCES

[1] J. Howard, *Americans Devote More Than 10 Hours a Day to Screen Time, and Growing.* https://www.cnn.com/2016/06/30/health/americans-screen-time-nielsen/index.html, 2018.

[2] C. Cajochen, S. Frey, D. Anders, J. Späti, M. Bues, A. Pross, R. Mager, A. Wirz-Justice, and O. Stefani, "Evening exposure to a light-emitting diodes (led)-backlit computer screen affects circadian physiology and cognitive performance," *Journal of Applied Physiology*, vol. 110, no. 5, pp. 1432–1438, 2011.

[3] L. Hale and S. Guan, "Screen time and sleep among school-aged children and adolescents: a systematic literature review," *Sleep medicine reviews*, vol. 21, pp. 50–58, 2015.

[4] T. Bedrosian and R. Nelson, "Timing of light exposure affects mood and brain circuits," *Translational psychiatry*, vol. 7, no. 1, p. e1017, 2017.

[5] F. Lin, Y. Zhou, Y. Du, L. Qin, Z. Zhao, J. Xu, and H. Lei, "Abnormal white matter integrity in adolescents with internet addiction disorder: a tract-based spatial statistics study," *PloS one*, vol. 7, no. 1, p. e30253, 2012.

[6] *The High Cost of Sleep Disorders.* https://thebenefitsguide.com/high-cost-sleep-disorders/, Accessed: 2018-11-16.

[7] *How to Manage Parental Control Over Your Child's Screen Time.* http://time.com/5260086/parental-controls-screen-time-app/, Accessed: 2018-11-21.

[8] M. Korayem, R. Templeman, D. Chen, D. Crandall, and A. Kapadia, "Enhancing lifelogging privacy by detecting screens," in *ACM CHI Conference on Human Factors in Computing Systems (CHI)*, 2016.

[9] C. Fan, Z. Zhang, and D. J. Crandall, "Deepdiary: Lifelogging image captioning and summarization," *Journal of Visual Communication and Image Representation*, 2018.

[10] I. Konig, P. Beau, and K. David, "A new context: Screen to face distance," in *Medical Information and Communication Technology (ISMICT), 2014 8th International Symposium on.* IEEE, 2014, pp. 1–5.

[11] Z. Li, W. Chen, Z. Li, and K. Bian, "Look into my eyes: Fine-grained detection of face-screen distance on smartphones," in *Mobile Ad-Hoc and Sensor Networks (MSN), 2016 12th International Conference on.* IEEE, 2016, pp. 258–265.

[12] A. J. McGonigle, T. C. Wilkes, T. D. Pering, J. R. Willmott, J. M. Cook, F. M. Mims, and A. V. Parisi, "Smartphone spectrometers," *Sensors*, vol. 18, no. 1, p. 223, 2018.

[13] M. A. Hossain, J. Canning, K. Cook, and A. Jamalipour, "Optical fiber smartphone spectrometer," *Optics letters*, vol. 41, no. 10, pp. 2237–2240, 2016.

[14] T. Matsumoto, S. Haga, T. Nakatsue, S. Kubota, Y. Kubota, K. Imabayashi, K. Kishimoto, S. Goshi, S. Imai, and Y. Igarashi, "Appropriate luminance of lcd-tv screens under actual viewing condition at home," in *Sony, SID Symposium Digest of Technical Papers (42)*, vol. 1, 2011, pp. 221–224.

[15] *Fluorescent lamp.* https://en.wikipedia.org/wiki/Fluorescent_lamp, Accessed: 2018-6-27.

[16] M. Collares-Pereira and A. Rabl, "The average distribution of solar radiation-correlations between diffuse and hemispherical and between daily and hourly insolation values," *Solar energy*, vol. 22, no. 2, pp. 155–164, 1979.

[17] D.-K. Yang, *Fundamentals of liquid crystal devices.* John Wiley & Sons, 2014.

[18] T. J. Bruno and P. D. Svoronos, *CRC handbook of fundamental spectroscopic correlation charts.* CRC Press, 2005.

[19] H. Curtis and N. S. Barnes, *Invitation to biology.* Macmillan, 1994.

[20] R. Hunt, "The reproduction of colour sixth edition," *John Wiley & Sons*, 2004.

[21] P. Dietz, W. Yerazunis, and D. Leigh, "Very low-cost sensing and communication using bidirectional leds," in *International Conference on Ubiquitous Computing.* Springer, 2003, pp. 175–191.

[22] S. Schmid, G. Corbellini, S. Mangold, and T. R. Gross, "An led-to-led visible light communication system with software-based synchronization," in *Globecom Workshops (GC Wkshps), 2012 IEEE.* IEEE, 2012, pp. 1264–1268.

[23] *Red LED.* https://www.sparkfun.com/datasheets/Components/LED/Red-10mm.pdf, Accessed: 2018-6-28.

[24] *Green LED.* https://www.sparkfun.com/datasheets/Components/LED/Green-10mm.pdf, Accessed: 2018-6-28.

[25] *Blue LED.* https://www.sparkfun.com/datasheets/Components/LED/Blue-10mm.pdf, Accessed: 2018-6-28.

[26] *LEDs are Photodiodes Too.* https://www.analog.com/en/analog-dialogue/raqs/raq-issue-108.html, year =Accessed: 2019-04-23.

[27] *Cree XLamp XM-L Color LEDs.* https://www.cree.com/led-components/media/documents/XLampXML_Color.pdf, year =Accessed: 2019-04-23.

[28] J. Ma, J. Chiles, Y. D. Sharma, S. Krishna, and S. Fathpour, "Two-photon photovoltaic effect in gallium arsenide," *Optics letters*, vol. 39, no. 18, pp. 5297–5300, 2014.

[29] S. Fathpour, K. K. Tsia, and B. Jalali, "Two-photon photovoltaic effect in silicon," *IEEE Journal of quantum electronics*, vol. 43, no. 12, pp. 1211–1217, 2007.

[30] *LED: COM-09592-YSL-R531K3D-D2.* https://www.sparkfun.com/datasheets/Components/LED/COM-09592-YSL-R531K3D-D2.pdf, year =Accessed: 2019-03-19.

[31] F. Cai, W. Lu, W. Shi, and S. He, "A mobile device-based imaging spectrometer for environmental monitoring by attaching a lightweight small module to a commercial digital camera," *Scientific reports*, vol. 7, no. 1, p. 15602, 2017.

[32] Y. Hayashi, N. Homma, M. Miura, T. Aoki, and H. Sone, "A threat for tablet pcs in public space: Remote visualization of screen images using em emanation," in *Proceedings of the 2014 ACM SIGSAC Conference on Computer and Communications Security.* ACM, 2014, pp. 954–965.

[33] *CdS Photoconductivity Cells.* https://cdn.sparkfun.com/datasheets/Sensors/LightImaging/SEN-09088.pdf, Accessed: 2018-6-28.

[34] *SDigital Red, Green and Blue Color Light Sensor with IR Blocking Filter.* https://cdn.sparkfun.com/datasheets/Sensors/LightImaging/isl29125.pdf, Accessed: 2018-6-29.

[35] *AS7263.* https://cdn.sparkfun.com/assets/1/b/7/3/b/AS7263.pdf, Accessed: 2018-6-28.

[36] *Silicon PIN Photodiode, RoHS Compliant.* https://www.sparkfun.com/datasheets/Prototyping/Solar/bpw34.pdf, Accessed: 2018-6-28.

[37] *TCS34725.* https://cdn-shop.adafruit.com/datasheets/TCS34725.pdf, year =Accessed: 2018-11-18.

[38] R. Amin, S. Knowlton, B. Yenilmez, A. Hart, A. Joshi, and S. Tasoglu, "Smartphone attachable, flow-assisted magnetic focusing device," *RSC Advances*, vol. 6, no. 96, pp. 93 922–93 931, 2016.

[39] B. Razavi, *Design of analog CMOS integrated circuits.* Tsinghua University Press Ltd., 2001.

[40] J. R. Macdonald and M. K. Brachman, "The charging and discharging of nonlinear capacitors," *Proceedings of the IRE*, vol. 43, no. 1, pp. 71–78, 1955.

[41] J. Moll, S. Krakauer, and R. Shen, "Pn junction charge-storage diodes," *Proceedings of the IRE*, vol. 50, no. 1, pp. 43–53, 1962.

[42] Z. Wang and D. Zhang, "Progressive switching median filter for the removal of impulse noise from highly corrupted images," *IEEE Transactions on Circuits and Systems II: Analog and Digital Signal Processing*, vol. 46, no. 1, pp. 78–80, 1999.

[43] A. C. Harvey, *Forecasting, structural time series models and the Kalman filter.* Cambridge university press, 1990.

[44] *Dell 24 Monitor: P2417H.* https://www.dell.com/en-us/shop/dell-24-monitor-p2417h/apd/210-aiim/monitors-monitor-accessories, Accessed: 2018-7-21.

[45] A. Wang, F. Lin, Z. Jin, and W. Xu, "Ultra-low power dynamic knob in adaptive compressed sensing towards biosignal dynamics," *IEEE transactions on biomedical circuits and systems*, vol. 10, no. 3, pp. 579–592, 2016.

[46] S. Xiong, S. Zhu, Y. Ji, B. Jiang, X. Tian, X. Zheng, and X. Wang, "iblink: Smart glasses for facial paralysis patients," in *Proceedings of the 15th Annual International Conference on Mobile Systems, Applications, and Services.* ACM, 2017, pp. 359–370.

[47] A. Mayberry, P. Hu, B. Marlin, C. Salthouse, and D. Ganesan, "ishadow: design of a wearable, real-time mobile gaze tracker," in *Proceedings of the 12th annual international conference on Mobile systems, applications, and services.* ACM, 2014, pp. 82–94.

[48] H. Feng, K. Fawaz, and K. G. Shin, "Continuous authentication for voice assistants," in *Proceedings of the 23rd Annual International Conference on Mobile Computing and Networking.* ACM, 2017, pp. 343–355.

[49] C. Cornelius, R. Peterson, J. Skinner, R. Halter, and D. Kotz, "A wearable system that knows who wears it," in *Proceedings of the 12th annual international conference on Mobile systems, applications, and services.* ACM, 2014, pp. 55–67.

[50] *Samsung Galaxy S9+.* https://www.samsung.com/global/galaxy/galaxy-s9/, Accessed: 2018-7-21.

[51] I. A. G. Duarte, M. d. F. S. Hafner, and A. A. Malvestiti, "Ultraviolet radiation emitted by lamps, tvs, tablets and computers: are there risks for the population?" *Anais brasileiros de dermatologia*, vol. 90, no. 4, pp. 595–597, 2015.

[52] R. M. Bolle, J. H. Connell, S. Pankanti, N. K. Ratha, and A. W. Senior, *Guide to biometrics.* Springer Science & Business Media, 2013.

[53] S. Zimmeck, J. S. Li, H. Kim, S. M. Bellovin, and T. Jebara, "A privacy analysis of cross-device tracking," in *26th USENIX Security Symposium (USENIX Security 17).* USENIX Association, 2017, pp. 1391–1408.

[54] C. M. Sommerich, S. M. Joines, and J. P. Psihogios, "Effects of computer monitor viewing angle and related factors on strain, performance, and preference outcomes," *Human factors*, vol. 43, no. 1, pp. 39–55, 2001.

[55] *Lighting Ergonomics-Survey and Solutions.* https://www.ccohs.ca/oshanswers/ergonomics/lighting_survey, Accessed: 2018-6-21.

[56] *Narrative.* http://getnarrative.com/, year =Accessed: 2018-11-19.

[57] V. Talla, M. Hessar, B. Kellogg, A. Najafi, J. R. Smith, and S. Gollakota, "Lora backscatter: Enabling the vision of ubiquitous connectivity," *Proceedings of the ACM on Interactive, Mobile, Wearable and Ubiquitous Technologies*, vol. 1, no. 3, p. 105, 2017.

[58] T. Li and X. Zhou, "Battery-free eye tracker on glasses," in *Proceedings of the 24th Annual International Conference on Mobile Computing and Networking.* ACM, 2018, pp. 67–82.

[59] Y. Li, T. Li, R. A. Patel, X.-D. Yang, and X. Zhou, "Self-powered gesture recognition with ambient light," in *The 31st Annual ACM Symposium on User Interface Software and Technology.* ACM, 2018, pp. 595–608.

[60] M. Yoshimura, M. Kitazawa, Y. Maeda, M. Mimura, K. Tsubota, and T. Kishimoto, "Smartphone viewing distance and sleep: an experimental study utilizing motion capture technology," *Nature and science of sleep*, vol. 9, p. 59, 2017.

[61] N. Charness, K. Dijkstra, T. Jastrzembski, S. Weaver, and M. Champion, "Monitor viewing distance for younger and older workers," in *Proceedings of the Human*

Factors and Ergonomics Society Annual Meeting, vol. 52, no. 19. SAGE Publications Sage CA: Los Angeles, CA, 2008, pp. 1614–1617.

[62] M. Ardito, "Studies of the influence of display size and picture brightness on the preferred viewing distance for hdtv programs," *SMPTE journal*, vol. 103, no. 8, pp. 517–522, 1994.

[63] *A Six-Point Checklist to Correctly Position Your Computer Monitor.* https://ergo-plus.com/office-ergonomics-position-computer-monitor/, Accessed: 2018-11-6.

[64] A. J. Das, A. Wahi, I. Kothari, and R. Raskar, "Ultra-portable, wireless smartphone spectrometer for rapid, non-destructive testing of fruit ripeness," *Scientific reports*, vol. 6, p. 32504, 2016.

[65] P. Edwards, C. Zhang, B. Zhang, X. Hong, V. K. Nagarajan, B. Yu, and Z. Liu, "Smartphone based optical spectrometer for diffusive reflectance spectroscopic measurement of hemoglobin," *Scientific reports*, vol. 7, no. 1, p. 12224, 2017.

[66] F. Wahl, J. Kasbauer, and O. Amft, "Computer screen use detection using smart eyeglasses," *Frontiers in ICT*, vol. 4, p. 8, 2017.

[67] *iOS 12 introduces new features to reduce interruptions and manage Screen Time.* https://www.apple.com/newsroom/2018/06/ios-12-introduces-new-features-to-reduce-interruptions-and-manage-screen-time/, Accessed: 2018-10-25.

[68] *Great technology should improve life, not distract from it.* https://wellbeing.google/, Accessed: 2018-11-15.

[69] Z. Tian, K. Wright, and X. Zhou, "The darklight rises: Visible light communication in the dark," in *Proceedings of the 22nd Annual International Conference on Mobile Computing and Networking*. ACM, 2016, pp. 2–15.

[70] Y. Yang, J. Nie, and J. Luo, "Reflexcode: Coding with superposed reflection light for led-camera communication," in *Proceedings of the 23rd Annual International Conference on Mobile Computing and Networking*. ACM, 2017, pp. 193–205.

[71] T. Rahman, A. T. Adams, P. Schein, A. Jain, D. Erickson, and T. Choudhury, "Nutrilyzer: A mobile system for characterizing liquid food with photoacoustic effect," in *Proceedings of the 14th ACM Conference on Embedded Network Sensor Systems CD-ROM*. ACM, 2016, pp. 123–136.

[72] S. Liu and T. He, "Smartlight: Light-weight 3d indoor localization using a single led lamp," in *Proceedings of the 15th ACM Conference on Embedded Network Sensor Systems*. ACM, 2017, p. 11.

[73] A. Wang, T. Wang, C. Zhou, and W. Xu, "Luban: Low-cost and in-situ droplet micro-sensing for inkjet 3d printing quality assurance," in *Proceedings of the 15th ACM Conference on Embedded Network Sensor Systems*. ACM, 2017, p. 27.

[74] S. Zhu, C. Zhang, and X. Zhang, "Automating visual privacy protection using a smart led," in *Proceedings of the 23rd Annual International Conference on Mobile Computing and Networking*. ACM, 2017, pp. 329–342.